ISSN: 2414-1895 DOI: 10.6919/ICJE.202205_8(5).0096

Single Image Dehazing based on Two-stage Optimal Fusion Method

Weina Zhou[a], Chengxiang Ouyang[b]

School of Shanghai Maritime University, Shanghai 201306, China

[a]wnzhou@shmtu.edu.cn, [b]chengxiangoy@163.com

Abstract

Fog is the result of the accumulation of dust and smoke particles in the air, which can lead to a decrease in the visibility and contrast of images, and has a huge impact on outdoor video surveillance, daily camera photography, and more. Based on the improved DCP algorithm, this paper proposes a new two-stage single image removal algorithm. The two stages are the optimization of the transmission map and atmospheric light, respectively. For the transmission map, a rough transmission map is obtained by weight fusion, which consists of sky and non-sky regions. The non-sky area is obtained by the improved dark channel algorithm based on the adaptive filter window, and the sky area is obtained by the classical color attenuation prior algorithm. Finally, a weighted fusion method is proposed to combine the transmission maps of the two regions, so that the intersection of the combined coarse transmission maps is more natural. For atmospheric light, we combine the advantages of the bright channel and propose to replace the global atmospheric light with the local atmospheric light value, so that the estimated atmospheric light can better reflect the real ocean environment. The experimental results show that the proposed dehazing algorithm can greatly improve the visibility of the image and effectively avoid the color distortion of the hazy image.

Keywords

Image Processing; Adaptive Filter Window; Bright Channel Prior; Atmospheric Scattering Model.

1. Introduction

With the deterioration of the current environment, smog has become a common weather phenomenon, and PM2.5 has become a common term in the public's mouth. The suspended particles in the smog will enter the lungs through the respiratory tract with human breathing. Physical and mental health pose a great threat. Smog is the result of the accumulation of dust and smoke particles in the air, which can lead to a decrease in the visibility and contrast of images, and has a huge impact on outdoor video surveillance, daily camera photography, and more. At the same time, fog and haze weather will also bring great benefits to many fields such as outdoor video surveillance, drone aerial patrols, daily camera photography, as well as existing vehicle, aircraft and ship safety assisted driving systems or future autonomous driving. hidden danger. Therefore, removing the influence of haze in the air by some means outdoors, obtaining high-quality clear images, and improving the reliability of the collected image data have become the focus of attention, and it has also become a difficult and hot spot for researchers to overcome.

In recent decades, many effective single-image defogging algorithms have been proposed. The image dehaing algorithms can be divided into two methods. The first method is the image enhancement

ISSN: 2414-1895 DOI: 10.6919/ICJE.202205_8(5).0096

algorithm, which does not take the physical imaging model into account. The algorithm of image enhancement mainly enhances the visual information of the image by enhancing the brightness and contrast of the image. Common algorithms such as histogram equalization[1], sharpening[2], wavelet transform[3], logarithmic transformation and so on. Retinex algorithm has the characteristics of local contrast enhancement and dynamic range compression. On the basis of Retinex, many scholars have improved it, such as the most classic retinex, such as SSR[4],MSR[5],MSRCR[6], etc. In general, the image defogging algorithm based on image enhancement is relatively simple and easy to understand in principle and does not need to estimate too many complex atmospheric parameters. However, the defogging effect is limited and the restoration results are not realistic enough.

The another method is image restoration algorithm based on physical model. Atmospheric scattering model is the core of defogging algorithm based on physical model. Through extensive studies, Nayer et al. systematically elaborated the mechanism of image information degradation in fog, and derived atmospheric scattering model, which laid a foundation for the research on fog removal based on physical model. At present, the research on defogging methods based on the physical model of atmospheric scattering can be divided into the following three categories: based on image depth information, based on the polarization characteristics of atmospheric light, and based on prior information. The method based on image depth information is to obtain the parameters of the image degradation model with fog image first , and then bring the parameters into the atmospheric scattering physical model to restore the fog-free image. Oakley et al.[7] estimated the scene depth and terrain model according to the flight parameters and radar information of the aircraft to recover the gray fog image captured by the aircraft airborne sensor. Tan et al.[8] combined the relation between wavelength and contrast degradation and extended this algorithm to color fogged images. Hautiere et al.[9] obtained the depth information to and from fog through the on-board optical sensing system and the three-dimensional geographic model. The defogging method based on the polarization of atmospheric light needs to be shot in the same scene with different degrees of polarization so as to obtain multiple images with different degrees of polarization. The atmospheric light is estimated by the difference between the two polarization degrees, and then the original fog-free image is recovered. As for the defogging method based on prior information As for the defogging method based on prior information, researchers analyze various physical models and make statistics and induction on a large number of foggy images, and obtain some prior assumptions to solve the problem of insufficient scene information provided by a single image. There are some well-known prior assumptions were proposed. For example, He et al.[10] proposed dack channel prior (DCP), pointed out that in most non-sky local areas, some pixels always have at least one color channel with very low, that is, the minimum value of light intensity in this area is a very small number; Dana Berman er al.[11] proposed non-local prior (NLP), and observe that pixels in a given cluster are often non-local; Through a large number of statistical studies, Zhu et al.[12] proposed color attenuation prior (CAP), and found that the variation of the brightness and saturation of pixels in foggy images were related to the concentration of fog in the image scene, and proposed that the difference between the brightness and saturation of foggy images was linearly related to the depth of field. Among these prior assumptions, the dark channel method proposed by He et al. has a significant impact. Although He's method can achieve better performance, the algorithm is time consuming, and it fails to deal with the bright white areas such as the sky. The main reason is they used soft-matting to optimize the transmission image. In order to improve the efficiency of He’s algorithm, guilded image filtering, joint bilateral filter, variational regularized (VR)[13], total generalized variation (TGV), image guided TGV, etc. were proposed to optimize the transmission image. Xu et al.[14] proposed the bright channel prior (BCP)[15] and observed that in most blurred images, some pixels will always have at least one color channel with greater intensity. that is, the intensity of the bright channel at a certain pixel point is close to the atmospheric light intensity of the fog-free image.

With the rapid development of deep learning, many researchers have applied the convolutional neural network (CNN) and its improved structure to image defogging. For example, DehazingNet[16], and U-net[13] were used to estimate the transmission image. Without estimating transmission map and

ISSN: 2414-1895 DOI: 10.6919/ICJE.202205_8(5).0096

atmospheric light individually, AOD-Net[17] and FEED-Net[18] adopt end-to-end design, and directly generates clear images through light-weight CNN. Although these deep learning networks can produce good defogging effect, the training time of the network is long, and the training results need a large number of sample data, and most of the existing training datasets are synthetic. Therefore the defogging effect of realistic fogging pictures is not better than that of some traditional algorithms. Moreover, the dataset of fog images under the Marine background studied in this paper is more difficult to obtain.

This paper proposes an improved single image dehazing method. First, to optimize the transmission image, a coarse transmission image is generated by weighted fusion of two different transmission images acquired from the foreground and sky regions. The foreground transmission image is generated by introducing an adaptive filter window to improve the dark channel algorithm, and the sky area is generated by the color attenuation prior. By fusing the two partial regions, the junction of the merged coarse transmission image is made more natural. For the optimization of atmospheric light, combined with the prior theory of the channel, the optimized atmospheric light value is obtained. Finally, using the atmospheric physical model and the two optimized atmospheric parameters obtained above, a clear restored image is obtained. Experiments show that our algorithm outperforms other state-of-the-art image dehazing algorithms and improves visibility better. The proposed algorithm is shown in Fig. 1.

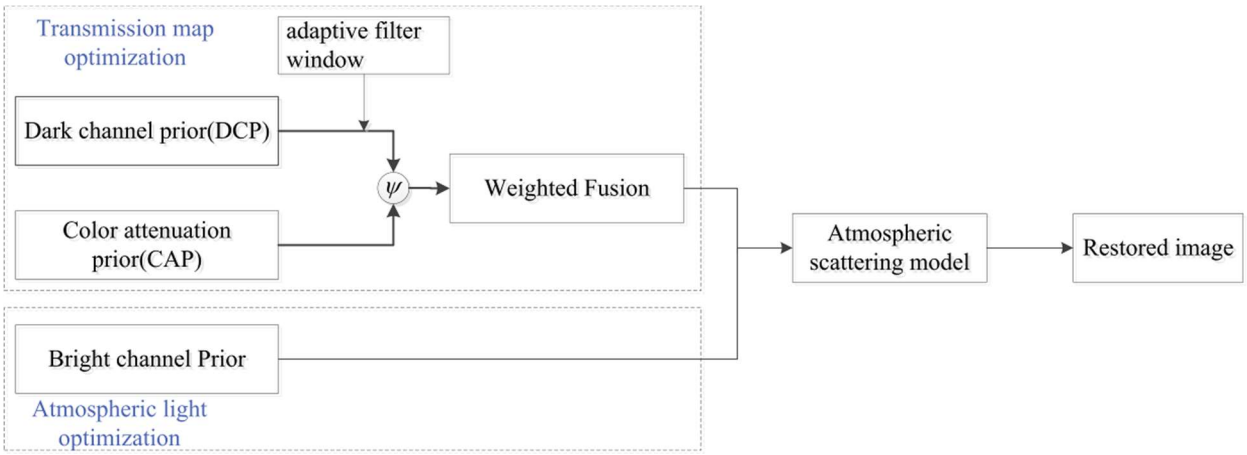

Fig. 1 The architecture of the proposed algorithm

2. Transmission Map Optimization Strategy

In the field of computer vision, a foggy image degradation model is usually used to describe the impact of haze and other severe weather conditions on images. This model was first proposed by McCartney[19]. The model includes two parts: attenuation model and ambient light model, and the expression can be showed as follows:

$$I(x) = J(x)t(x) + A(1 - t(x)) \tag{1}$$

where $I(x)$ is the observed hazy image, $J(x)$ is fog-free image or scene reflection, $t(x)$ is transmission map, A is the global atmospheric light, which generally considered to be the highest intensity pixel in an image, and x is pixel coordinate of the image. In fact, all defogging algorithms are based on the known foggy image $I(x)$ to obtain the transmission map $t(x)$ and the global atmospheric light A. Therefore, the algorithm proposed in this paper will optimize the two parameters of transmission map and atmospheric light to achieve a better dehazing effect.

ISSN: 2414-1895 DOI: 10.6919/ICJE.202205_8(5).0096

2.1 Improved Dark Channel Algorithm based on Adaptive Filter Window

In the previous content, we concluded that the atmospheric scattering model can be expressed by Eq.1, and Eq.1 can be expressed in the following normalized form:

$$\frac{I^c(x)}{A^c} = t(x)\frac{J^c(x)}{A^c} + 1 - t(x) \tag{2}$$

where c stands for each individual color channel $c(r,g,b)$. In the dark channel algorithm, the minimum filtering with local region (x) is carried out on both sides of Eq.2, and the transmission map within this local region is assumed to be constant, which can be obtained as follows:

$$\min_{y\in\Omega(x)}(\min_{c\in(r,g,b)}\frac{I^c(y)}{A^c}) = t(x)\min_{y\in\Omega(x)}(\min_{c\in(r,g,b)}\frac{J^c(y)}{A^c}) + 1 - t(x) \tag{3}$$

It's known by a dark channel priori that:

$$\min_{y\in\Omega(x)}(\min_{c\in(r,g,b)}\frac{J^c(y)}{A^c}) = 0 \tag{4}$$

Combined with Eq.3 and Eq.4, we can get:

$$t(x) = 1 - \min_{y\in\Omega(x)}(\min_{c\in(r,g,b)}\frac{I^c(y)}{A^c}) \tag{5}$$

Although the dark channel algorithm achieves better defogging effect, it also has some limitations. An important drawback is that in the dark channel algorithm, a fixed rectangular window is used as the local filtering region, and the transmission map in the rectangular neighborhood window is assumed to be the same. According to the atmospheric scattering model, the transmittance is related to the depth of the scene, and satisfying the following relation:

$$t(x) = e^{-\beta d(x)} \tag{6}$$

where β is the dielectric scattering coefficient, and $d(x)$ is the depth of the scene. Therefore, the fixed neighborhood window selected by the dark channel may contain multiple depths of field, resulting in inconsistent transmittance in the window, which makes the transmission map estimated by the dark channel algorithm inaccurate.

This paper proposes an adaptive filtering window strategy, which determines the filtering window according to the size of the image. This method can effectively adaptively obtain the filter window size of dark channel images for images of different sizes, thereby improving the accuracy of transmission map estimation. The transmission graph expression of the dark channel algorithm using the adaptive filter window is improved as follows:

$$t_1(x) = 1 - \omega\min_{y\in S(x)}(\min_{c\in(r,g,b)}\frac{I^c(y)}{A^c}) \tag{7}$$

ISSN: 2414-1895 DOI: 10.6919/ICJE.202205_8(5).0096

$$w_{ad} = clamp\left(round\left(min\left(w\times 3\%, h\times 3\%\right)\right), 15, 32\right) \tag{8}$$

Where w_{ad} denotes the adaptive filter window, ω is the parameter to adjust the degree of defogging, usually 0.95.

2.2 Coarse Transmission Map Acquisition based on Weighted Fusion

Generally, the sea fog image has a large sky area. If the DCP algorithm is directly used, the image processing in the sky part will fail and halo effect will exist. Zhu et al.[20] found that the brightness and saturation of foggy images are related to the concentration of fog in the image scene through the statistics of a large number of foggy pictures. Due to the superposition effect of fog in the atmospheric environment, the fog concentration indirectly reflects the depth of field information in the image scene. The greater the depth of field, the greater the fog concentration. Therefore, Zhu et al. proposed that the difference between brightness and saturation of foggy images has a linear relationship with depth of field, and the expression is:

$$d(x,y) = \theta_0 + \theta_1 v(x,y) + \theta_2 s(x,y) \tag{9}$$

where $v(x,y)$ and $s(x,y)$ are brightness and saturation values at pixel point (x,y) respectively, θ_x is the coefficient, and its values are $\theta_0 = 0.121779$, $\theta_1 = 0.959710$, $\theta_2 = -0.780245$. Fig. 2 shows the changes of saturation, brightness, and the difference between saturation and brightness with the depth of field for a sea fog image. It can be seen from the change curve in Fig-4 that when the depth of field value is large, the linear relationship is obvious.

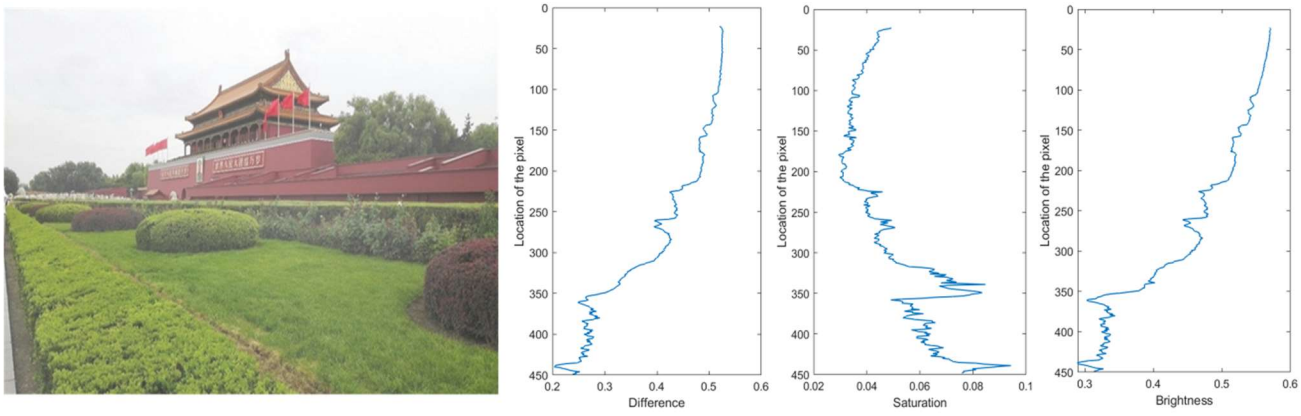

Fig. 2 Input image and image brightness, saturation changes with the depth of the scene. (a) An input fog image; (b) The difference between brightness and saturation; (c) The relationship between saturation and scene depth; (d) The relationship between brightness and scene depth

In order to correct the transmission map $t_1(x)$ in the sky region obtained by SSDCP algorithm in the previous section, the linear relationship in Eq.8 is used to get the transmission map $t_2(x) = e^{-\beta d(x)}$. The final coarse transmission map is $\overline{t}$ acquired by weightedly fusing t_1 and t_2. $\overline{t}$ is express as follows:

ISSN: 2414-1895 DOI: 10.6919/ICJE.202205_8(5).0096

$$\overline{t(x)} = \psi(x)t_1(x) + (1-\psi(x))t_2(x) \tag{10}$$

where the weight $\psi \in [0,1]$. If the pixel is in the non-sky region, ψ is tend to 1. On the contrary, if the pixel is in sky region, ψ is tend to 0. In this way, $\psi(x)$ will fuse the non-sky region of the transmission map t_1 and the sky region of the transmission map t_2 to obtain a more accurate transmission map $\overline{t}$.

3. Atmospheric Light Optimization Strategy

Similar to the dark channel prior, the basic idea of the bright channel prior is based on the statistical observation of a large number of foggy images and found that in the most of fuzzey images, some of the pixels had greater intensity in at least one color channel[21].The bright channel prior theory points out that the intensity of the bright channel at pixel x tends to be close to the atmospheric light intensity of the fog-free image. For any image I, its bright channel expression is:

$$I^{light}(x) = \max_{c\in\{r,g,b\}} [\max_{y\in S(x)} I^c(y)] \to A^{light}(x) \tag{11}$$

where $I^c(y)$ is a certain color channel of $\{r,g,b\}$ for image I.

Fig. 3 shows the dark channel and bright channel images of several sea fog images. It can be seen from Fig. 3 that the dark channel value of the foggy image in the non-sky area is very small and tends to 0, while the intensity of the bright channel tends to the atmospheric light intensity of the fog-free image.

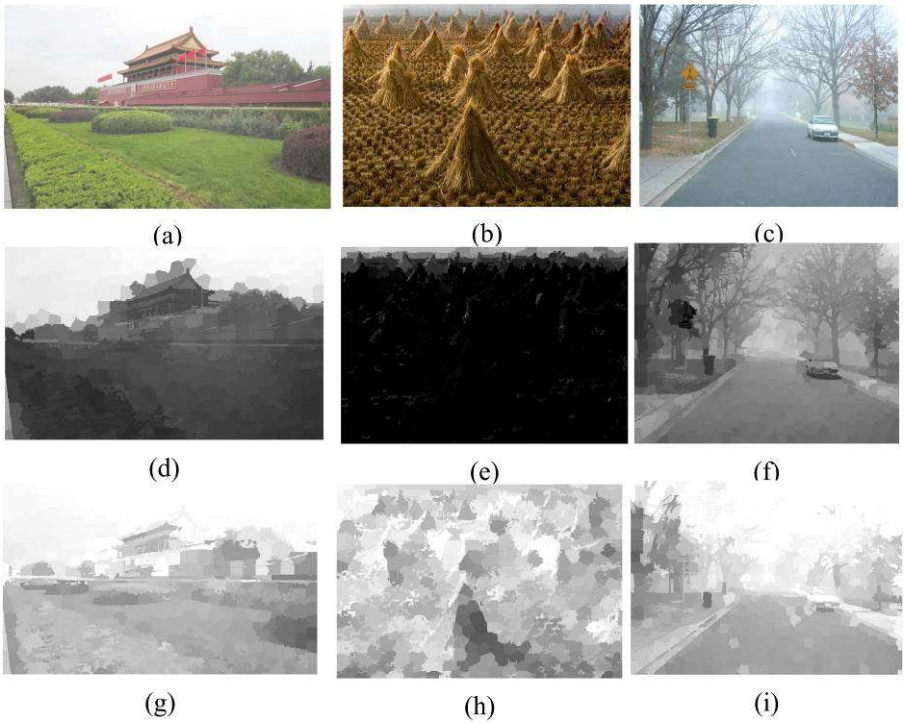

Fig. 3 Dack channel and bright channel images. (a)(b)(c) are the original images; (d)(e)(f) are the dack channel images; (g)(h)(i) are the bright channel images

In the dark channel prior algorithm, the method to determine the atmospheric light value is to select the pixel with the first 0.1% brightness in the dark channel image and then correspond the location of

ISSN: 2414-1895 DOI: 10.6919/ICJE.202205_8(5).0096

the pixel to the original foggy image, and finally, select the highest value of brightness as atmospheric light A. However, since there is generally a large area of sky in the sea fog image, the atmospheric light directly selected in this way will appear deviation and a large number of color spots in the image after processing. In this paper, we propose an optimization method for atmospheric light value combining the bright channel prior. The atmospheric light is expressed as follows:

$$A(x) = A^{light}(x) \tag{12}$$

Based on the optimized transmission map $t(x)$ and the atmospheric light value $A(x)$ obtained above, the fog-free image can be restored by the atmospheric scattering model. The restored clear image can be expressed as:

$$J(x) = \frac{I(x) - A(x)}{\max(t(x), \tilde{t})} + A(x) \tag{13}$$

where $\tilde{t}$ is a set parameter to avoid introducing noise when the transmittance is too small. Usually, $\tilde{t}$ is set to 0.1.

4. Experimental Result and Analysis

In this section, some experiments are executed to verify the effectiveness and suitability of the proposed method in visual maritime detection. Our method is compared with the algorithms of DCP[10], MSR[22], CAP[13] from the aspect of visual effects and objective quality assessment. The experimental parameters in this paper are respectively set to: $\lambda_1 = 0.25$, $\lambda_2 = 1$, $\lambda_3 = 0.5$, $\lambda_4 = 0.3$, β_1, $\beta_2 = 0.5$, $\beta_3 = 0.55$. The images are selected from the dataset set up by Hu et al.[24]. The proposed algorithm is tested using MATLAB2014b on a desktop computer with 8G memory and a 2.5GHz processor.

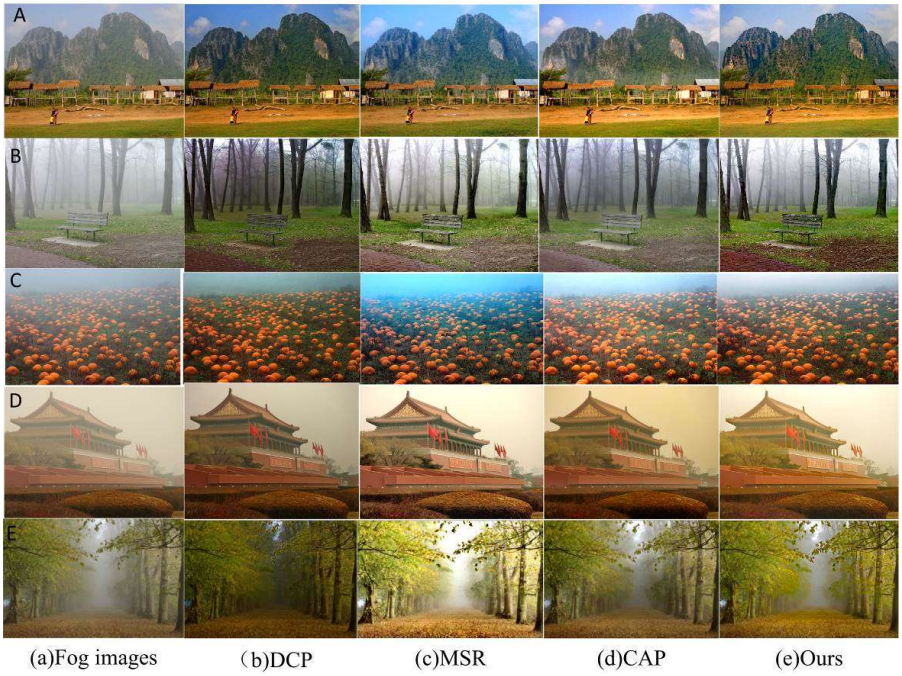

Fig. 4 Results of different defogging methods. (a)Original fog images, (b)DCP method, (c) MSR method, (d)CAP method, (e)Our method

ISSN: 2414-1895 DOI: 10.6919/ICJE.202205_8(5).0096

Dfogging results of five methods above are shown in Fig.4. By comparison, it can be found that the images in Fig. 4(a) show obvious color distortion in the sky area, and there is a halo phenomenon in the connection between the sky and the non-sky area; Although images in Fig.4(b) can remove most of the sea fog, the exposure in the sky area is serious, making the overall color brighter. In Fig.4(c), the defogging effect is visually dark overall. In Fig.4(d), color distortion also appears in the sky area, the overall contrast is too high, and the defogging effect is not obvious for images with heavy fog. The results in Fig.4(e) show that our method is in a more realistic visual effect, and most of the sea fog can be removed.

Evaluate the results of the above methods based on objective indicators, we used the blind defogging assessment by gradient rationing at visible edges[23-25]. The blind assessment criteria contains three quantitative metrics, including the rate of new visible edges e, the average gradient ratio $\bar{r}$ and the ratio of saturated pixels σ. They are calculated by:

$$e = \frac{n_r - n_0}{n_0} \tag{14}$$

$$\bar{r} = \exp[\frac{1}{n_r} \sum_{P_i \in \wp_r} \log r_i] \tag{15}$$

$$\sigma = \frac{n_s}{\dim_x \times \dim_y} \tag{16}$$

Table 1. The three quantitative metrics of the five defogging methods

Image	Evaluation	DCP	MSR	CAP	Ours
	e	4.1274	4.5311	1.6675	**6.2049**
Figure(A)	$\bar{r}$	2.5743	2.9049	2.1965	**3.4093**
	σ(%)	0	7.6296	0	0
	e(%)	0.7753	0.7941	0.4453	**1.8490**
Figure(B)	$\bar{r}$	2.4984	2.5080	1.9847	**3.9114**
	σ(%)	0.0039	2.9128	0	0.01341
	e(%)	2.4090	**2.6823**	1.0785	3.1168
Figure(C)	$\bar{r}$	2.6649	4.0720	2.1748	**4.5599**
	σ(%)	0	6.5877	0	0.0094
	e(%)	0.7907	0.6221	0.43692	**1.9032**
Figure(D)	$\bar{r}$	1.7602	3.9460	1.6480	**4.6243**
	σ(%)	0.0028	1.7620	0	0.00142
	e(%)	2.8101	**3.3858**	1.4987	3.0633
Figure(E)	$\bar{r}$	2.4748	**5.1515**	2.1853	4.4445
	σ(%)	0	1.6549	0	0.0218

ISSN: 2414-1895 DOI: 10.6919/ICJE.202205_8(5).0096

Where n_0 and n_r denote the number of visible edges in the original image and in the restored image.

P_i and $\wp_r$ are the pixel of visible edge and the set of the visible edges in the restored image. Where $\dim_x$ and $\dim_y$ denote the width and the height of the image. Among these indicators, the higher the e and $\bar{r}$, the better defogging efficacy. And the smaller σ, the better the color restoration effect. Table 1 shows the quantitative metrics of Figs. A-E via five defogging methods above.

Table 1 shows that, in Figure (C) and Figure (E), although the index value of the algorithm proposed by us is smaller than that of the MSR algorithm, it can be seen from Fig-6(d) that the processing result of the MSR algorithm is over-enhanced, especially the halo phenomenon exists in the sky area, and the overall effect is lower than the processing result of the proposed method. In general, the algorithm proposed in this paper has improved on these three indicators compared with the other four algorithms.

In conclusion, no matter from the perspective of subjective visual evaluation or objective evaluation index, the algorithm proposed by us is better than the above other defogging algorithms in the processing of sea fog images, and it has an important breakthrough in the problem of visual image detection.

5. Conclusion

Aiming at the shortcomings of the original dehazing algorithm, this paper proposes a simple and effective sea fog dehazing algorithm. We start with an atmospheric model and optimize for transmission maps and atmospheric light values. For the transmission map, we fuse the transmission map of the sky area and the non-sky area by simple weights. The transmission map of the non-sky area is obtained by introducing an adaptive filter window and improved DCP algorithm, and the transmission map of the sky area is obtained by the CAP algorithm. picture. Finally, the two parts of the transmission graph are fused by a certain weight. For atmospheric light, since the sea fog image has a large bright white area, we combine the advantages of the bright channel and propose to replace the global atmospheric light with the local atmospheric light value, so that the estimated atmospheric light can better reflect the real environment. The experimental results show that the proposed dehazing algorithm can greatly improve the visibility of the image and effectively avoid the color distortion of the image, so the proposed dehazing algorithm has important application value in visual inspection. However, the algorithm still has some defects, and the dehazed image still has the influence of noise. In future work, we will further study denoising, perform real-time image dehazing, etc.

Acknowledgments

This study was supported by the National Natural Science Foundation of China (Grant No. 52071200, 61404083).

References

[1] Land, Edwin H. The Retinex Theory of Color Vision[J]. Scientific American, 1977, 237(6):108-128.

[2] Doo Hyun Choi; Ick Hoon Jang; Mi Hye Kim. Color Image Enhancement Based on single-scale Retinex With a JND-Based Nonlinear Filter[C]. IEEE International Symposium on Circuits and Systems, 2007.

[3] Jobson D J, Rahman Z, Woodell G A. Multiscale retinex for bridging the gap between color images and the human observation of scenes[J]. IEEE Transactions on Image Processing, 1997, 6(7):965-976.

[4] Z.Rahman, D.J.Jobson, G.A.Woodell, Multiscale retinex for color rendition and dynamic range compression, in Proceedings of SPIE2847, Society of Photo-Optical Instrumentation Engineers Press, Bellingham, 1996, pp. 183–191.

[5] S. G. Narasimhan and S. K. Nayar, Contrast restoration of weather degraded images, IEEE Transactions on Pattern Analysis and Machine Intelligence, vol. 25, no. 6, pp. 713-724, Jun. 2003.

ISSN: 2414-1895 DOI: 10.6919/ICJE.202205_8(5).0096

[6] J.B. Wang, N.He, L.L.Zhang, et al., Single image dehazing with a physical model and dark channel prior, Neurocomputing 149(2015)718–728.

[7] Nayar S K, Narasimhan S G. Vision in Bad Weather[C]// Seventh IEEE International Conference on Computer Vision. 2002.

[8] He K, Jian S, Tang X. Single image haze removal using dark channel prior[C] IEEE Conference on Computer Vision & Pattern Recognition. 2009.

[9] Berman, D., Treibitz, T., & Avidan, S. (2016). Non-local Image Dehazing. In: Computer Vision and Pattern Recognition. Las Vegas. pp:1674-1682.

[10] Zhu Q S, Mai J M, Shao L. A Fast Single Image Haze Removal Algorithm Using Color Attenuation Prior[J]. IEEE Trans. on Image Processing. 2015-24(11): 3522-3533.

[11] K. He, J.Sun, X.Tang, Guided image filtering, Pattern Anal. Mach. Intell. 35(6) (2013)1397–1409.

[12] L. Chen, B.L.Guo, J.Bi, et al., Algorithm of single image fog removal based on joint bilateral filter, J.Beijing Univ. Posts Telecommun. 35(4)(2012)19–23.

[13] Zhou W, Zhou Y. An attention nested U-Structure suitable for salient ship detection in complex maritime environment[J]. IEICE Transactions on Electronics, Vol.E105-D,No.6,pp.-,Jun. 2022.

[14] Q. Shu, C. Wu, R. W. Liu, et al., Two-phase transmission map estimation for robust image dehazing, in Proc. ICONIP, Siem Reap, Cambodia, Dec. 2018, pp. 529-541.

[15] Cai, B., Xu, X., Jia, K., Qing, C., & Tao, D. (2016). DehazeNet: An End-to-End System for Single Image Haze Removal. IEEE Transactions on Image Processing, 25(11), 5187-5198.

[16] W. Ren, S. Liu, H. Zhang, J. Pan, X. Cao, and M. H. Yang, Single image dehazing via multi-scale convolutional neural networks, in Proc. ECCV, Amsterdam, The Netherlands, Oct. 2016, pp. 154-169.

[17] B. Li, X. Peng, Z. Wang, J. Xu, and D. Feng, Aodnet: All-in-one dehazing network, in Proc. IEEE ICCV, Venice, Italy, Oct. 2017, pp. 4780-4788.

[18] S. Zhang, W. Ren, and J. Yao, FEED-Net: Fully end-to-end dehazing, in Proc. IEEE ICME, San Diego, CA, USA, Oct. 2018, pp. 1-6.

[19] E. J. McCartney, Optics of the atmosphere, Science Press, 1988.

[20] Jiang Y T Sun C M Zhao Y, et al., Image dehazing using adaptive bi-channel priors on superpixels[J[, Computer Vision and Image Understanding 2017,165, 17-32.

[21] Achanta R, Shaji A, Smith K, et al., SLIC superpixels compared to state-of-the-art superpixel methods[J]. IEEE Transactions on Pattern Analysis and Machine Intelligence, 2012, 34(11): 2274-2282.

[22] Duo Qiu; Hu Zhu; Xiongjun Zhang, An Implementable Accelerated Alternating Direction Method of Multipliers for Low-Rank Tensor Completion, 2018 IEEE International Conference on Internet of Things, 2018.

[23] Xu Y, Guo X, Wang H, et al. Single image haze removal using light and dark channel prior [C], IEEE International Conference on Communications in China, 2016: 1- 6.

[24] Hai-Miao Hu, Qiang Guo, Jin Zheng, et al., Single Image Defogging Based on Illumination Decomposition for Visual Maritime Surveillance. 2019.

[25] N. Hautiere, J.P. Tarel, D. Aubert, et al., Blind contrast enhancement assessment by gradient rationing at visible edges, Image Anal. Stereol[J]. 27 (2) (2008)87–95.